

## Pressure Dependence of Ionic Conductivity in KCl, NaCl, KBr, and NaBr<sup>†</sup>

D. N. Yoon\* and D. Lazarus

*Department of Physics and Materials Research Laboratory, University of Illinois, Urbana, Illinois 61801*

(Received 24 January 1972)

The pressure dependence of the ionic conductivity of KCl, NaCl, KBr, and NaBr has been measured to 6 kbar in the intrinsic and extrinsic temperature regions. In the intrinsic region the conductivity deviates markedly from a simple exponential decrease with pressure. A detailed analysis, including contributions from anions and extrinsic cation vacancies, shows that pressure can suppress the intrinsic vacancies sufficiently to cause such a deviation. The analysis also shows that the uncertainties in the estimated activation volumes are greater than those determined in previous work. For KCl, NaCl, KBr, and NaBr crystals, respectively, the estimated activation volumes for motion of cation vacancies are  $8 \pm 1$ ,  $7 \pm 1$ ,  $11 \pm 1$ , and  $8 \pm 1$  cm<sup>3</sup>/mole, and the activation volumes for formation of Schottky defects are  $61 \pm 9$ ,  $55 \pm 9$ ,  $54 \pm 9$ , and  $44 \pm 9$  cm<sup>3</sup>/mole. The values for activation volumes of motion agree with predictions of the strain-energy model of Keyes. Schottky-defect-formation volumes are substantially larger than the molar volumes in KCl and NaCl, but in KBr and NaBr they are approximately equal.

### I. INTRODUCTION

It is fairly well established that ionic conduction in alkali halides occurs through movement of vacancies. From the pressure dependence of the conductivity  $\sigma$ , the activation volumes associated with vacancy creation and motion can be estimated. In the extrinsic region the number of cation vacancies is more or less fixed by the polyvalent-cation impurity content, and the pressure dependence of  $\sigma$  gives the activation volume  $\Delta V_m^*$  associated with motion of cation vacancies. In the intrinsic region, where Schottky defects are predominant, the pressure dependence of  $\sigma$  is associated with the sum of formation and motion volumes. Within the usual assumptions of reaction-rate theory, the formation volume of Schottky defects can be estimated by subtracting  $\Delta V_m^*$  from the total activation volume determined in the intrinsic region.

Many theoretical calculations of the activation energy for vacancies are also concerned with the activation volume, since they are closely related. Both atomic and continuum strain-energy models have been used to calculate the volume of motion.<sup>1</sup> In the dynamical theory of diffusion suggested recently by Flynn,<sup>2,3</sup>  $\Delta V_m^*$  does not represent any physical change of volume during the atomic migration, but is related to the change of optical-mode frequencies with pressure.

The activation volume for formation calculated for Schottky defects is very sensitive to the nature of the models and approximations used. In several previous calculations, the degree of lattice relaxation and its relationship to the formation volume have not been resolved satisfactorily. In ionic crystals both electrostatic and elastic forces contribute to the lattice relaxation, and the formation volume is not related to the relaxation of the near-

est-neighbor atoms around vacancies in a simple way. The recent theory of Faux and Lidiard<sup>4</sup> appears to represent a significant advance, but their results do not agree with values deduced from pressure measurements.

Previously, several experimental investigations have been made of the pressure dependence of the ionic conductivity of KCl and NaCl. Biermann<sup>5</sup> measured the pressure dependence of conductivity of KCl and NaCl in the intrinsic and extrinsic ranges to 0.5 kbar. The pressure dependence of the extrinsic conductivity was measured to higher pressures by Pierce<sup>6</sup> in KCl and NaCl and by Taylor *et al.*<sup>7</sup> in KCl. Recently, Beyeler and Lazarus<sup>8,9</sup> made measurements in the intrinsic and extrinsic ranges in NaCl to 6 kbar. Some previous work has indicated that, in the intrinsic range, the conductivity does not, in fact, decrease exponentially with pressure and this deviation is due to the extrinsic vacancies.<sup>9,10</sup>

In the previous analysis of experimental results, it was assumed that in the intrinsic region only cations contribute to the conductivity. Recent results, however, indicate that the anions contribute significantly to the intrinsic conduction near the melting point. In addition, the contribution of the extrinsic vacancies should be included even in the intrinsic region, since intrinsic vacancies can be suppressed by application of high pressure (because of the large value of  $\Delta V_f$ ). Inclusion of these effects may indicate that the pressure variation of the ionic conductivity is not as simple as previously thought and that the uncertainties in the activation volumes are greater.

Furthermore, it is desirable to extend the measurements to KBr and NaBr to determine any possible correlation between the activation volumes and the type of anion in alkali-halide crystals. In

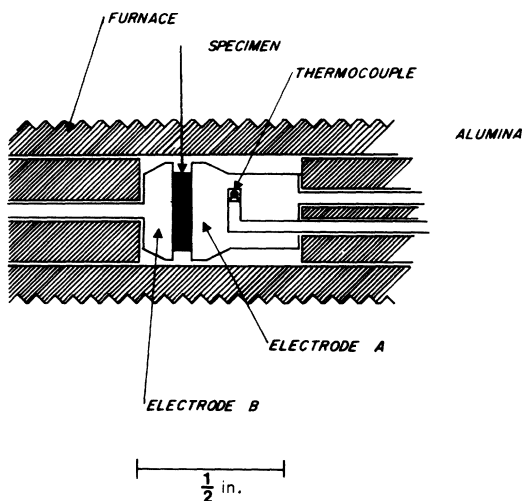


FIG. 1. Electrode, thermocouple, and furnace assembly for conductance measurement.

this paper we present the results of our observations of the pressure dependence of the ionic conductivity of KCl, NaCl, KBr, and NaBr in the intrinsic and extrinsic regions at pressures to 6 kbar. Activation volumes are estimated using a model which includes contributions of the anion and the extrinsic vacancies to the conductivity. The results are compared with various theoretical predictions.

## II. EXPERIMENTAL TECHNIQUES AND PROCEDURES

The basic gas-pressure system used in these measurements consists of commercially available equipment, and the details have been previously described.<sup>11</sup> Argon gas of 99.995% purity was used as a pressure medium. The bomb had inside dimensions of  $1\frac{5}{8}$ -in. diameter and 9-in. length. Thermocouple and electrical leads were brought out with no discontinuities through U-shaped pressure tubings containing frozen oil. Pressure was measured with a Heise 100 000 psi bourdon gauge with an accuracy of better than 1%. The piston in the separator was designed to ensure complete separation of gas from oil. The piston was a little longer than half the inside length of the separator, and both ends were packed with Bridgman-type "T" pieces.

A cylindrical platinum-wound alumina furnace was placed inside the bomb. The furnace core had uniformly spaced grooves for the heating wires. At each end of the furnace smaller size wires were used for a few turns to obtain a flat temperature region over a 2-in. center zone with about 1 °C per in. gradient at 700 °C.

The electrode and sample assembly is shown in Fig. 1. The electrodes were made of nickel with platinum sheets brazed onto their contact faces.

Two features of this assembly should be noted. First, there was about a  $\frac{1}{32}$ -in. gap between the inner wall of the furnace core and the electrode faces, so that any spurious conductance through the furnace wall or transfer of any contaminant on it to the specimen would be reduced. Secondly, the chromel-alumel thermocouple was inserted deeply into the massive electrode A, and its end was bent parallel to the electrode contact face. To achieve this, electrode A was made of two parts. The thermocouple was insulated with alumina tubing, and the tip was cemented to the electrode with Sauereisen cement. These procedures were followed in order to ensure a good thermal contact between the thermocouple and the electrode. Previous results have shown<sup>10,12</sup> that it is essential to maintain good thermal contact between the thermocouple and a specimen to obtain accurate specimen temperature measurements. In addition, a temperature calibration was obtained between the measuring thermocouple in electrode A and a second thermocouple inserted through electrode B and sandwiched between two halves of a KCl sample. The difference between temperatures measured by these two couples decreased sharply with pressure from about 3 or 4 °C at low pressures to about 1 °C at 0.7 kbar<sup>13</sup> and remained constant at higher pressures. These small corrections were applied to the measured ionic conductivity.

The electrode contact faces were ground flat and smooth. In order to improve the specimen-electrode contact, the electrodes were pressed against the specimen by spring tension and were heated close to the melting point of the specimen before commencing measurements. Although this technique does not ensure perfect contacts, it was previously shown<sup>14</sup> that errors due to imperfect contacts can be overcome by using a high-frequency signal in the ac bridge. In this work, conductance and capacitance were often measured at varying frequencies to check the possible space-charge effect arising from imperfect contacts. In general, frequencies of 5 to 10 kHz were sufficiently high. A Boonton model No. 750 bridge was used for the conductivity measurements. Although the accuracy of this bridge specified by the manufacturer is not high (about 10%), the values obtained showed about 2% random difference from those measured with a General Radio No. 716-C bridge (2% rated accuracy). Therefore, the absolute error due to the bridge in the measured conductivity is believed to be about 4%.

The undoped "pure" specimens were obtained from the Harshaw Chemical Company. The samples containing divalent impurities were grown by the Kyropoulos method with a circulating argon atmosphere. The grown crystals were slowly cooled to room temperature. Typical sample di-

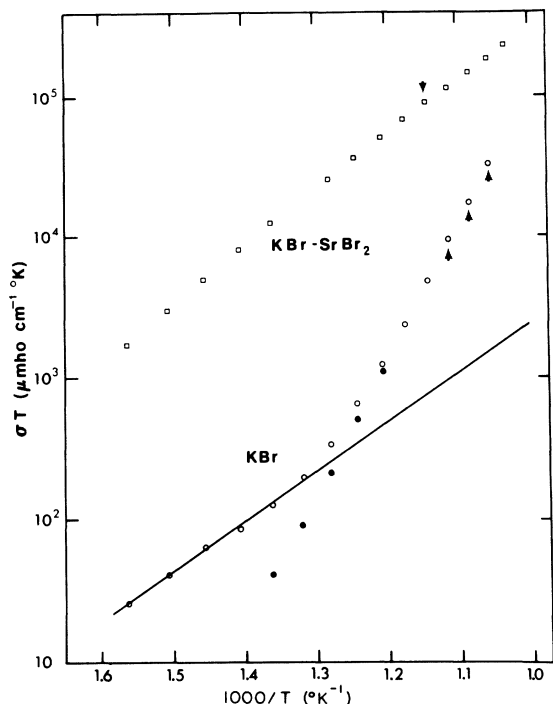


FIG. 2. Observed temperature dependence of conductivities in "pure" and Sr-doped KBr single crystals; closed circles indicate initial heating.

mensions were  $0.5 \times 0.5 \times 0.15$  cm.

The most important potential error in this type of measurement is that arising from spurious conductance. This can arise from impurities, such as

a carbon deposit across the electrodes or between the electrical leads coming out of the pressure vessel. In order to check such effects, the conductance across the electrodes was measured without any sample and also with a dummy alumina ring over the entire pressure and temperature range used in the experiment. The spurious conductance never exceeded 0.05% at the sample conductance. During the measurements, samples were sometimes left at high temperature and pressure for long times to detect possible contamination effects increasing with time. In addition, data were taken with several cycles of pressure. No systematic increase of the conductance with time was observed in the high-temperature intrinsic region.

### III. RESULTS

Figure 2 shows the observed temperature dependence of the conductivities for single crystals of Harshaw "pure" KBr and KBr doped with Sr. These measurements were made in the pressure vessel with about 0.5-kbar pressure. Chemical analysis and comparison with the previous measurements indicate about  $2 \times 10^{-4}$  mole fraction of Sr in the doped sample. The conductivity of "pure" samples at low temperatures showed marked dependence on the thermal treatment of the sample. During the initial heating, the conductivity (closed circles) is low, extending the apparent intrinsic region to low temperatures. However, once the sample has been heated to a temperature close to the melting point, there is a marked increase in conductivity (open circles) at low temperatures, shifting the knee to higher temperatures. Similar behavior is found

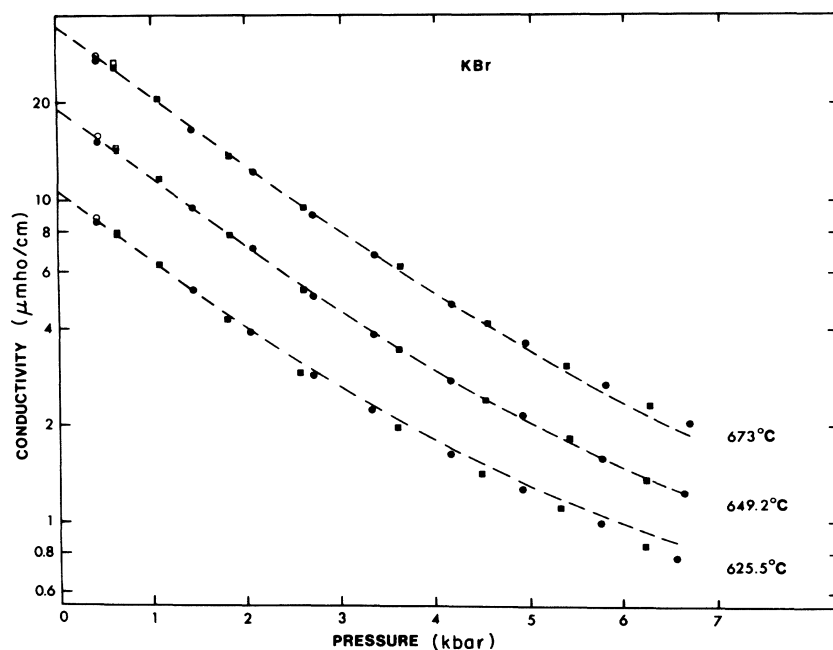


FIG. 3. Pressure dependence of conductivity in "pure" KBr in the intrinsic temperature range. Dashed lines show theoretical fit (see text); open symbols indicate data points without temperature correction.

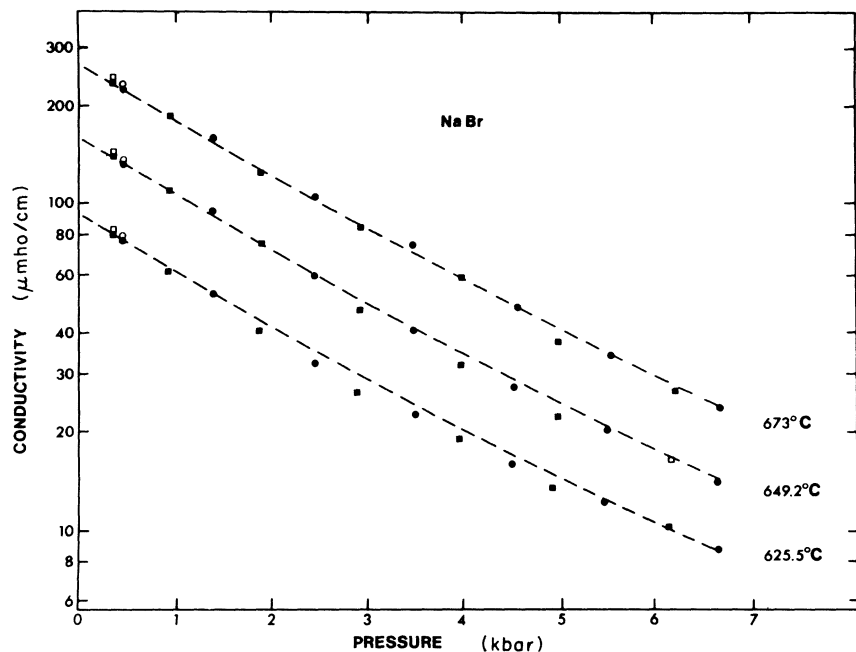


FIG. 4. Pressure dependence of conductivity in "pure" NaBr in the intrinsic temperature range. Dashed lines show theoretical fit (see text); open symbols indicate data points without temperature correction.

for KCl, NaCl, and NaBr. These shifts of the knee are believed to be caused by the presence of  $\text{OH}^-$  ions in the crystals, and will be discussed later. The knee temperature of the Harshaw crystals determined from the temperature dependence of the conductivity measured *after* the pressure runs agreed well with previous results on Harshaw crystals.<sup>8,15,16</sup> The arrows indicate the temperature at which pressure measurements were made.

The pressure dependence of the conductivity for Harshaw KBr, NaBr, KCl, and NaCl crystals is

shown in Figs. 3–6. The temperatures correspond to the "intrinsic" region at zero pressure. At low pressures the open circles and squares represent values before applying the temperature correction discussed earlier. One important feature of these results is that, at high pressures, the rate of decrease in conductivity with pressure is reduced, as indicated by the slight curvatures in these figures. The pressure range at which the curvature begins to appear tends to shift to lower pressures as the temperature is decreased. The dotted lines show

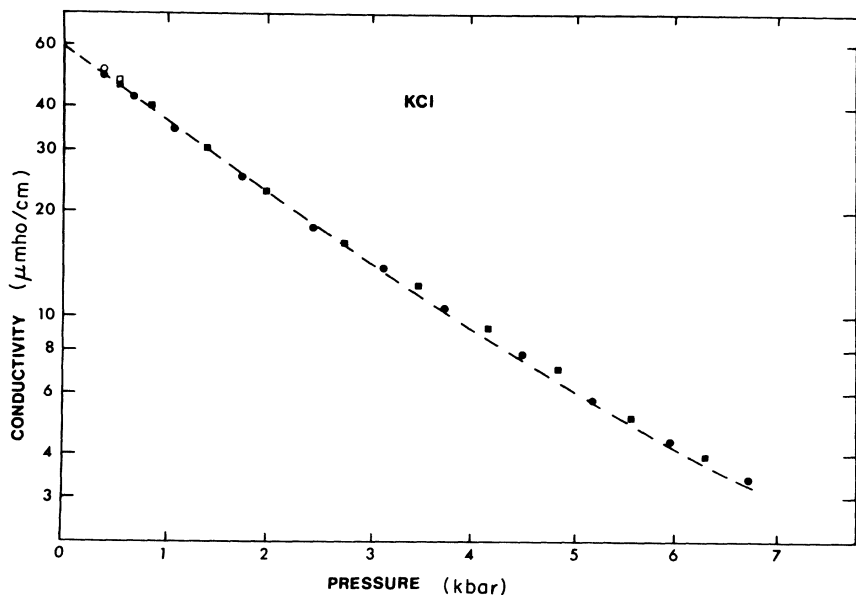


FIG. 5. Pressure dependence of conductivity in "pure" KCl in the intrinsic temperature range at 704°C. Dashed lines show theoretical fit (see text); open symbols indicate data points without temperature correction.

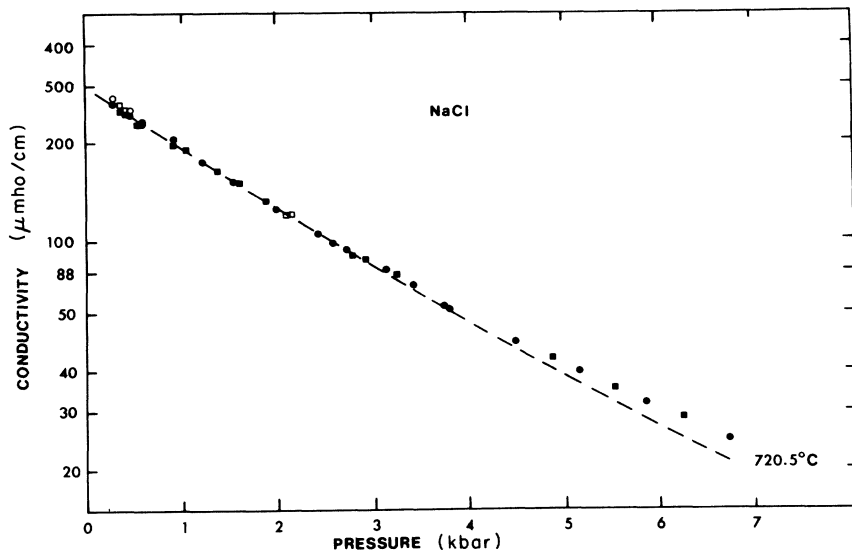


FIG. 6. Pressure dependence of conductivity in "pure" NaCl in the intrinsic temperature range. Dashed line shows theoretical fit (see text); open symbols indicate data points without temperature correction.

a numerical fit to the curves based on a model which will be discussed later.

Figure 7 shows the observed pressure dependence of the conductivity of KBr doped with Sr (KBr-Sr). KCl-Sr, NaCl-Ca, and NaBr-Ca showed similar behavior. A slight deviation from exponential dependence occurs at low pressures. Such an effect may be due to the greater contribution from the intrinsic vacancies at low pressures. Therefore, the data below 1 kbar were ignored in evaluating the activation volumes of motion.

#### IV. DISCUSSION

##### A. Comparison with Previous Measurements

Before evaluating the activation volumes and discussing their significance, it is desirable to compare our results with the previous measurements on the pressure dependence of the intrinsic conductivity. Since our  $\ln\sigma$ -vs.-pressure plots show curvatures at high pressures, we first confine our attention to the low-pressure regions below 3 kbar

where  $\sigma$  follows a simple exponential decrease.

The values of  $\partial\ln\sigma/\partial P$  shown in Table I were obtained from the data at pressures below 3 kbar and the highest measurement temperatures for each sample. The errors shown are due to the uncertainty in the temperature correction at low pressures and the standard deviation in evaluating the slope. Table I also shows the results of Biermann<sup>5</sup> and Beyeler and Lazarus<sup>6</sup> for comparison. All the results in this table were obtained at temperatures between 680 and 720 °C. Although Biermann<sup>5</sup> does not indicate his uncertainties, it is possible that the discrepancy with our results is due to his limited pressure range (0–0.5 kbar) and the subsequent large random error expected in  $\partial\ln\sigma/\partial P$ .

The disagreement between the present results and that of Beyeler and Lazarus<sup>6</sup> is more serious, because it is clear that random errors cannot account for such a large difference. Moreover, Beyeler and Lazarus's results show a linear decrease of  $\ln\sigma$  with pressure for the entire pressure

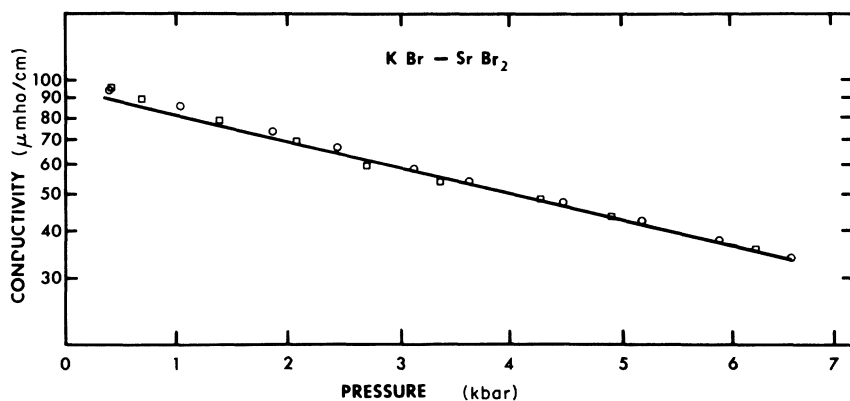


FIG. 7. Observed pressure dependence of the extrinsic conductivity in KBr doped with Sr at 602 °C.

range between 0 and 6 kbar, whereas our results show curvature in the high-pressure region.

One possible reason for the curvature is the presence of a large amount of divalent cations or other impurities. However, the "knee" temperature in Beyeler-Lazarus data for NaCl is exactly the same as ours measured after completing the pressure measurements, indicating that our NaCl sample did not contain or gain any more impurity than Beyeler and Lazarus's. In addition, the larger value for  $-(\partial \ln \sigma / \partial P)$  in our measurements (at low pressures) is inconsistent with the possibility of larger amounts of impurities in our sample.

Another possible reason for such a systematic discrepancy is errors in the temperature measurement. As explained earlier, considerable effort was taken to reduce the temperature errors in the present experiment. Therefore, it is unlikely that the temperature errors in our measurements were great enough to cause this discrepancy or the curvature at high-pressure regions.

In the Beyeler-Lazarus<sup>8,9</sup> experiment there was a large pressure-dependent discrepancy between the temperature measured by their measuring thermocouple and that indicated by a second thermocouple buried inside their (considerably thicker) specimen. Fairly large corrections were thus required, particularly in the low-pressure ranges where the discrepancy is greatest. On the other hand, Beyeler and Lazarus repeated their measurements in the low-pressure range (0–0.8 kbar) at temperatures up to 670 °C using an *externally* heated pressure vessel, where uncertainties in temperature should have been minimized. They found the same value of  $\partial \ln \sigma / \partial P$  for this case, but there is some possibility that these later samples may have been slightly contaminated by impurities diffusing in from the hot pressure vessel. In addition, the maximum temperature for this case (943 °K) was considerably lower than in the present measurement on NaCl (993 °K). As shown in Figs. 3 and 4 for KBr and NaBr, the average slopes of the  $\ln \sigma$ -vs-pressure plots decrease significantly with decreasing temperature, so the curvature may well have been obviated in the Beyeler-Lazarus experiment with the externally heated vessel.

Spurious conductivity is another possible source of error. In our measurements, as explained earlier, the spurious conductivity was shown to be negligibly small. In addition, curvatures of about the same degree were found in all our specimens in spite of the order-of-magnitude difference between the conductivities in the sodium and potassium halides at the same temperature. This observation provides further indirect evidence that spurious conductivity was not the cause of the curvature.

We have, therefore, no obvious reasons for

doubting our results and believe that the curvatures in the  $\ln \sigma$ -vs-pressure plots represent real effects in these samples. As discussed later, such curvature is expected for specimens containing even quite small concentrations of polyvalent impurities.

#### B. Calculation of Activation Volumes

Following the usual procedure, the activation volumes associated with motion and creation of vacancies can be calculated from the observed pressure dependence of the ionic conductivity. In the extrinsic region where the conduction is due solely to the cation motion, the reaction-rate theory gives<sup>17</sup>

$$\sigma = \frac{4n^+ e^2 a^2 \nu}{kT} e^{-\Delta G_m^*/kT}, \quad (1)$$

where  $e$  is the electronic charge,  $a$  is the lattice parameter,  $\nu$  is an atomic vibration frequency of the order of the Debye frequency,  $k$  is Boltzmann's constant,  $T$  is the absolute temperature, and  $\Delta G_m^*$  is the change in Gibbs free energy associated with the motion of a cation.  $n^+$  is the concentration of cation vacancies, which is fixed by the concentration of the divalent impurities if divalent impurity-vacancy complexes are negligible. The activation volume for motion is given by

$$\Delta V_m^* = \left( \frac{\partial \Delta G_m^*}{\partial P} \right)_T, \quad (2)$$

$$\Delta V_m^* = kT \left[ \left( \frac{\partial \ln a^2 \nu}{\partial P} \right)_T - \left( \frac{\partial \ln \sigma}{\partial P} \right)_T \right],$$

where  $\Delta V_m^*$  is the activation volume associated with the motion of a cation. The term  $(\partial \ln a^2 \nu / \partial P)_T$  can be estimated from the compressibility<sup>18–21</sup> and the pressure dependence of the elastic constants.<sup>21–23</sup> Its contribution to  $\Delta V_m^*$  is quite small, of the order of 2 to 5%.

Table II shows the estimated activation volumes for motion, along with the results of previous measurements on KCl and NaCl. Since our samples contained about the same amount of divalent ions as Pierce's,<sup>6</sup> about 10% correction was applied to account for divalent impurity-vacancy complexes in accordance with Pierce's analysis. Our values of  $\Delta V_m^*$  for KCl and NaCl agree well with those of Pierce.<sup>6</sup>

TABLE I. Observed pressure dependence of conductivity  $\partial \ln \sigma / \partial P$ , in KCl and NaCl from various measurements.

	NaCl (kbar <sup>-1</sup> )	KCl (kbar <sup>-1</sup> )
Present work	$-0.43 \pm 0.02$	$-0.49 \pm 0.02$
Biermann (Ref. 5)	-0.39	-0.55
Beyeler and Lazarus (Ref. 8)	-0.33	...

In the "intrinsic" region for "pure" crystals, the calculation of the activation volume is simplified if the following assumptions are made: First, the contribution of the extrinsic vacancies to the conduction is negligible, and second, only cations contribute to the conductivity. With these assumptions, the conductivity is given by<sup>17</sup>

$$\sigma = \frac{4e^2 a^2 \nu}{kT} \exp\left(-\frac{\Delta G_m^* + \frac{1}{2} \Delta G_f}{kT}\right), \quad (3)$$

where  $\Delta G_f$  is the Gibbs free energy associated with formation of an isolated pair of cation and anion vacancies (Schottky defect). The pressure dependence of  $\sigma$  is purely exponential and gives

$$\Delta V_t = \Delta V_m^* + \frac{1}{2} \Delta V_f = kT \left[ \left( \frac{\partial \ln a^2 \nu}{\partial P} \right)_T - \left( \frac{\partial \ln \sigma}{\partial P} \right)_T \right], \quad (4)$$

where  $\Delta V_f$  is the activation volume associated with formation of an isolated pair of cation and anion vacancies. Therefore,  $\Delta V_f$  can be estimated by subtracting  $\Delta V_m^*$  from  $\Delta V_t$ .

Anticipating that the first assumption of purely intrinsic conduction would be more applicable at low pressures and high temperatures, Eq. (4) was applied to the data (Figs. 3-6) at the highest temperatures and at pressures below 3 kbar, where  $\sigma$  shows a purely exponential decrease with pressure. In Table III, the third column [ $\Delta V_f(1)$ ] shows the values of  $\Delta V_f$  calculated in this manner. Our derived values of  $\Delta V_m^*$  were used. The uncertainties noted for  $\Delta V_f$  include the effects of the random errors in determining the slopes of the  $\ln \sigma$ -vs-pressure plots, the uncertainty in temperature calibration discussed earlier, and the uncertainties in  $\Delta V_m^*$ .

A more accurate estimate of the activation volume in the intrinsic region must include contributions from anion motion and the presence of extrinsic cation vacancies. It has been shown recently<sup>24-26</sup> that in these alkali-cation halides the anion contribution to the conduction at high temperatures is significant. The extrinsic cation vacancies also cannot be ignored at high pressures, because increasing pressure would have a similar effect as decreasing temperature, in sharply suppressing the concentration of intrinsic Schottky defects.

An expression for ionic conductivity which includes the anion and extrinsic vacancy contributions can be obtained by a simple extension of the reaction-rate theory. In this more general case,  $\sigma$  is given by<sup>17</sup>

$$\sigma = Ne(X^+ \mu^+ + X^- \mu^-), \quad (5)$$

where  $N$  is the number of ions per unit volume,  $X^+$  and  $X^-$  are the mole fractions of cation and anion vacancies, and  $\mu^+$  and  $\mu^-$  are their mobilities. The pressure and temperature dependences are given by

$$\begin{aligned} X^+ &= \frac{1}{2} c [(1 + 4 X_0^2 / c^2)^{1/2} + 1], \\ X^- &= \frac{1}{2} c [(1 + 4 X_0^2 / c^2)^{1/2} - 1], \\ X_0 &= e^{-\Delta G_f / 2kT}, \\ \mu^+ &= \frac{4a^2 e \nu}{kT} e^{-\Delta G_m^+ / kT}, \\ \mu^- &= \frac{4a^2 e \nu}{kT} e^{-\Delta G_m^- / kT}, \end{aligned} \quad (6)$$

where  $c$  is the mole fraction of divalent cation impurity. These relationships are based on the assumption that divalent impurities do not form complexes or precipitates with other species such as the cation vacancies or  $\text{OH}^-$  ions which might be present. In particular, Eqs. (5) and (6) allow the possibility that at extremely high pressures the intrinsic vacancies are suppressed by pressure and the systems reach the "extrinsic" region with a decreasing slope in the  $\ln \sigma$ -vs-pressure relationship.

Assuming further that  $\Delta V_f$  decreases with pressure in the same way as the total bulk volume, the pressure dependence of  $\sigma$  is easily shown to be derivable from the following equations:

$$\begin{aligned} \sigma &= A(1 - KP)^{2/3} \nu(P) \\ &\times \left( (B+1)e^{-P\Delta V_m^+ / kT} + (B-1) \frac{\mu_0^+}{\mu_0^-} e^{-P\Delta V_m^- / kT} \right), \\ B &= \left( 1 + \frac{4X_0'^2}{c^2} e^{-P\Delta V_f(1-KP) / kT} \right)^{1/2}. \end{aligned} \quad (7)$$

Here  $A$  is an adjustable constant determined from the observed value of  $\sigma$  at zero pressure and a

TABLE II. Observed activation volumes for motion of cations in alkali halides (in  $\text{cm}^3/\text{mole}$ ).

	Present work	Pierce (Ref. 6)	Biermann (Ref. 5)	Taylor <i>et al.</i> (Ref. 7)	Beyeler and Lazarus (Ref. 8)
KCl	$8 \pm 1$	$7.7 \pm 0.5$	10	8.6	...
NaCl	$7 \pm 1$	$7.0 \pm 0.5$	9.5	...	$6.6 \pm 0.6$
KBr	$11 \pm 1$	...	...	...	...
NaBr	$8 \pm 1$	...	...	...	...

specific temperature,  $X'_0$  is the value of  $X_0$  at zero pressure,  $\mu_0^+$  and  $\mu_0^-$  are mobilities at zero pressure, and  $K$  is the isothermal compressibility. Using Eq. (7), the pressure dependence of  $\sigma$  was calculated, assuming various values of  $\Delta V_f$  (increasing in increments of  $0.5 \text{ cm}^3/\text{mole}$ ), and the value which gave the best fit to the data obtained at the highest temperature at pressures below 5 kbar was chosen. Above 5 kbar the curvatures become prominent, and the pressure dependence of  $\sigma$  is strongly influenced by several factors whose values are not accurately known. Therefore, in evaluating  $\Delta V_f$  the low-pressure data are still more significant.

The pressure dependence of  $\sigma$  calculated in this manner is shown in Figs. 3-6 along with the observed data. The calculated values of  $\Delta V_f$  are shown in the fourth column of Table III [ $\Delta V_f(2)$ ]. These values are close to those [ $\Delta V_f(1)$ ] determined from a simpler model which neglects the contributions of anions and extrinsic vacancies to the conductivity. The major difference is in the larger uncertainty in  $\Delta V_f(2)$ . In addition, as shown in Figs. 3-6, the  $\ln\sigma$ -vs.-pressure plots calculated by Eq. (7) show curvature at high pressures.

The large uncertainty in this analysis based on Eq. (7) arises because the values of many of the parameters in Eq. (7) are not accurately known. Therefore, a systematic computer calculation was carried out to determine the influence of each term in Eq. (7) on the curvature and the uncertainty in  $\Delta V_f$ .

First, as mentioned earlier, it was assumed that under compression  $\Delta V_f$  decreases with pressure in the same way as the total or molar volume. Inclusion of this effect causes only about 2% change in  $\Delta V_f$  from the value estimated at zero pressure. However, the contribution to the curvature in the  $\ln\sigma$ -vs.-pressure relationship is significant because of the fairly high compressibility of alkali halides at high temperature.<sup>18-21</sup>

Secondly, the ratios between the anion and cation mobilities  $\mu_0^-/\mu_0^+$  have not been accurately determined. Since in the high-temperature intrinsic region the number of anion and cation vacancies are almost equal,  $\mu_0^-/\mu_0^+$  is almost equal to  $t^-/t^+$ , where  $t^-$  and  $t^+$  are the transport numbers. However, values of  $t^-/t^+$  vary greatly from one measurement to another.<sup>17, 24-26</sup> Hence, the uncertainties in  $\mu_0^-/\mu_0^+$  are quite large and cause about 2% uncertainty in  $\Delta V_f$ .

Third, the values of  $\Delta V_m^-$  have not yet been determined experimentally. In the absence of an accepted theory for  $\Delta V_m^-$ , we assume that  $\Delta V_m^-/\Delta V_m^+$  would fall between unity and  $(r^-/r^+)^3$ , where  $r^-$  and  $r^+$  are the ionic radii. For these estimates the values suggested by Tosi and Fumi were used<sup>27</sup>; this uncertainty in values for  $\Delta V_m^-$  causes about a

4% uncertainty in  $\Delta V_f$ . With these values for  $\Delta V_m^-$ , inclusion of the anion contribution to the conductivity causes a negligible curvature in the  $\ln\sigma$ -vs.- $P$  plots. However, if values of  $\Delta V_m^-$  are much larger than those assumed here, the anion contribution will cause a larger curvature and reduce the estimated values for  $\Delta V_f$ .

The final and most important term is the ratio of the number of intrinsic vacancies to divalent (extrinsic) vacancies,  $X'_0/c$ . A reasonable first estimate of this term in the intrinsic region can be made by extrapolating the extrinsic conductivity to higher temperatures as shown in Fig. 2. Since the product of mobility and temperature is expected to show an exponential temperature dependence,  $X'_0/c$  will be equal to the ratio of the intrinsic conductivity to the extrapolated value of the extrinsic conductivity, if only the cations contribute to conduction.

The estimate of  $X'_0/c$ , however, is expected to be too large (or the estimated number of extrinsic vacancies too small) for two reasons. First, the anion contribution to the intrinsic conduction is significant. Secondly, the presence of  $\text{OH}^-$  ions strongly suppresses the number of extrinsic vacancies present at low temperatures by forming complexes with the divalent cations. Fritz, Luty, and Anger<sup>28</sup> have shown that the extrinsic conductivity of KCl crystals doped with KOH depends very strongly on annealing and treatment with chlorine. It was suggested that  $\text{OH}^-$  ions form a precipitate with Ca, effectively neutralizing the Ca ions. The difference between the extrinsic conductivities in quenched and annealed samples indicates that at high temperatures near the melting point, these  $\text{OH}^-$  and Ca complexes break up, restoring the full effect of the divalent impurities. Therefore, if  $\text{OH}^-$  ions were introduced into the crystal during growth or exposure to the atmosphere, the number of extrinsic vacancies in the intrinsic region would be much higher, by a factor of 2 or 3, than the value obtained by extrapolation of the observed low-temperature extrinsic conductivity. Since the anion contribution and the effect of  $\text{OH}^-$  ions cannot be accurately estimated, we assumed that  $X'_0/c$  would fall between one and three times the ratio of the observed intrinsic and extrapolated extrinsic conductivities. The large uncertainty in  $X'_0/c$ , however, causes only 4% uncertainty in  $\Delta V_f$ , since only our low-pressure data were fitted to the numerical results of Eq. (7).

As expected, introduction of the  $X'_0/c$  term accounting for the contribution of extrinsic vacancies greatly affects the curvature at high pressures. In fact, the curvatures indicated by the dotted lines in Figs. 3-6 were due mostly to the effect of the extrinsic vacancies. A smaller contribution to the curvature results from  $\Delta V_f$  itself decreasing with



TABLE III. Activation volumes for formation of Schottky defects compared to the molar volumes  $V_M$  at 700 °C (in cm<sup>3</sup>/mole).

Material	$V_M$	Present work			Biermann (Ref. 5)		Beyeler and Lazarus (Ref. 8)	
		$\Delta V_f(1)$	$\Delta V_f(2)$	$\Delta V_f(2)/V_F$	$\Delta V_f$	$\Delta V_f/V_m$	$\Delta V_f$	$\Delta V_f/V_m$
KCl	41.4	64 ± 5	61 ± 9	1.5 ± 0.2	67	1.6	...	...
NaCl	29.7	56 ± 5	55 ± 9	1.9 ± 0.3	43	1.5	39 ± 3	1.3 ± 0.1
KBr	47.6	54 ± 5	54 ± 9	1.1 ± 0.2	...	...	...	...
NaBr	35.4	46 ± 5	44 ± 9	1.2 ± 0.3	...	...	...	...

pressure, as discussed earlier.

The terms  $(1 - KP)^{2/3}$  and  $\nu(P)$  were treated in the same way as discussed earlier and have negligible effect on the uncertainties in  $\Delta V_f$  or the curvature. The remaining contributions to the uncertainty in  $\Delta V_f$  came from the random errors in fitting the observed data and the uncertainties in the temperature correction. These last effects contribute only about half the total uncertainty. We thus believe that our indicated limits of error shown in Table III [ $\Delta V_f(2)$ ] are far more realistic estimates of the total experimental and theoretical uncertainties involved in deducing values for the Schottky defect formation volume than the smaller limits suggested by earlier workers.

#### V. COMPARISON WITH THEORY

In the reaction-rate theory, which is based on the assumption of thermodynamic equilibrium throughout the diffusional process, the activation volume for motion,  $\Delta V_m$ , represents a real change in the crystal volume due to the presence of diffusing atoms at the energy saddlepoint. In this theory, calculations of  $\Delta V_m$  have been based either on atomic or continuum models.<sup>1</sup> In the atomic model the defect properties are calculated from assumed forms for the interatomic potentials. It has been previously pointed out<sup>1</sup> that in KCl and NaCl the values for  $\Delta V_m^+$  predicted by the atomic-model calculations are only about half the observed values.

The continuum model of Zener<sup>29</sup> and Keyes<sup>1</sup> assumes that the defect properties can be represented by the distortion of the macroscopic-crystal continuum. In this "strain-energy" model,  $\Delta V_m$  is given by

$$\Delta V_m = \left[ \left( \frac{\partial \ln C}{\partial P} \right)_T - K_T \right] \Delta G_m, \quad (8)$$

where  $K_T$  is the isothermal compressibility and  $\Delta G_m$  is the Gibbs free energy for motion.  $C$  is the effective shear modulus, which is related to the usual elastic constants by<sup>30</sup>

$$C = \frac{3}{5} C_{44} + \frac{1}{5} (C_{11} - C_{12}).$$

Using the most recent experimental data for  $K_T$ ,<sup>18-21</sup>  $\Delta G_m^+$ ,<sup>31</sup> and  $(\partial \ln C / \partial P)_T$ ,<sup>21-23</sup> values of  $\Delta V_m^+$  were

calculated from Eq. (8). The results are shown in the third column of Table IV. Since the relevant temperature is around 500 °C rather than room temperature, values of  $K_T$  at 500 °C were used. Only room-temperature values of  $(\partial \ln C / \partial P)_T$  are available. As shown in Table IV, these calculated values of  $\Delta V_m^+$  agree well with our observed values. It appears, therefore, that the strain-energy model provides a satisfactory calculation of  $\Delta V_m^+$  in these alkali halides.

On the other hand, Keyes<sup>1</sup> previously concluded that Eq. (8) is not quite satisfied for the alkali halides. He used the Grüneisen relation rather than the directly measured values of  $(\partial \ln C / \partial P)$ . Therefore, his calculated values for  $\Delta V_m^+$  were smaller than those given in the present and Pierce's<sup>6</sup> analysis. In addition, Biermann's<sup>5</sup> experimental values of  $\Delta V_m^+$  quoted by Keyes are larger than those of more recent measurements, as shown in Table II. Keyes's conclusion, therefore, appears to have been based on questionable data.

A different interpretation of  $\Delta V_m$  is provided by the dynamic theory of diffusion suggested by Rice and others,<sup>32</sup> and more recently expanded by Flynn.<sup>2,3</sup> In this model the activation volume for motion is a useful parameter to represent the pressure change of migration rates, but it does not correspond to any real volume change during a diffusion jump. Rather,  $\Delta V_m$  is closely related to the effect of pressure on the optical-mode lattice vibrations. Flynn obtains<sup>3</sup> the expression

$$\Delta G_m = \frac{1}{2} w^2 q^2,$$

TABLE IV. Comparison between experimental and calculated values for activation volumes of motion (in cm<sup>3</sup>/mole).

	$\Delta V_m$ (expt)	$\Delta V_m$ (calc) <sup>a</sup>	$\Delta V_m$ (calc) <sup>b</sup>
NaCl	7 ± 1	5 ± 1	...
KCl	8 ± 1	6 ± 1	23 ± 2
NaBr	8 ± 1	9 ± 1	...
KBr	11 ± 1	9 ± 1	24 ± 2

<sup>a</sup>Calculated from the strain-energy model using Eq. (8). (See text.)

<sup>b</sup>Calculated from Eq. (9) based on the dynamic theory. (See text.)

$$\Delta V_m = 2 \left( \frac{\partial \ln w}{\partial P} \right) \Delta G_m, \quad (9)$$

where  $w$  is the optical-mode frequency and  $q$  is a critical fluctuation parameter. For monatomic crystals, using the Debye approximation, Flynn regains the result of the strain-energy model Eq. (8).

Values of  $\Delta V_m^+$  were calculated from Eq. (9) using the experimentally determined pressure change of long-wavelength transverse-optic-mode frequencies.<sup>33</sup> The results, shown in the fourth column of Table IV, do not agree with our observation. It cannot be concluded, however, that Flynn's theory gives an incorrect result, since only the long-wavelength transverse mode was considered in our analysis, whereas the short-wavelength longitudinal-optic modes should dominate in the diffusion process.

Theoretical calculations of the volume of formation of the Schottky defects in ionic crystals have been previously performed along with calculations of the defect energy.<sup>34</sup> While the predicted defect energies show some agreement with experiment, the volumes of formation of defects are very sensitive to the nature of the models and approximations and in general do not agree with the observed pressure dependence of the conductivity.

A significant result of recent theoretical analysis is that the activation volume associated with formation of Schottky defects is not simply related to the relaxation of the nearest-neighbor atoms around vacancies. Rather, the relaxation of atoms far away from the defect has to be considered. Therefore, one cannot simply conclude that the nearest-neighbor atoms around vacancies relax outward if  $\Delta V_f$  is larger than  $V_M$ .

The most recent calculation by Faux and Lidiard<sup>4</sup> predicts that  $\Delta V_f$  (calculated at room temperature) is considerably smaller ( $\Delta V_f/V_M \sim 0.5$ ) than the molar volume  $V_M$ . This is in conflict with the results of our measurements, which show that  $\Delta V_f$  is greater than  $V_M$  in these alkali halides. Although it has been suggested<sup>3,4</sup> that anharmonic effects may cause the formation volume to increase with temperature, it is not presently obvious how such an effect will be great enough to resolve the discrepancy.

It should be noted that the experimentally determined values for  $\Delta V_f/V_M$  are considerably greater in the chlorides than in the bromides. Although the current theories cannot explain this difference, it may be related to the larger size of the bromide ions. It would be desirable to make similar measurements in the fluorides and iodides to determine

if this trend persists.

## VI. CONCLUSIONS

The ionic conductivities of "pure" Harshaw KCl, NaCl, KBr, and NaBr in the "intrinsic" temperature range do not show a simple exponential decrease with pressure between 0 and 6 kbar. The observed  $\ln \sigma$ -vs-pressure graphs show curvatures at high pressures. This curvature is most probably due to the presence of divalent cation impurities; the intrinsic Schottky defects are suppressed by pressure, and at higher pressures the relative contribution of the extrinsic cation vacancies to conduction will be increased. Thus the observed "pressure-knee" effect is apparently analogous to the "temperature knee" which separates the intrinsic from the extrinsic conduction region. At pressures beyond 6 kbar, one should approach the "extrinsic" region, and the pressure dependence of the conductivity will be further reduced. Our analysis also shows that the curvature can be caused partly by the decrease of  $\Delta V_f$  with pressure. An additional contribution to the curvature could arise from the anion, especially if the activation volume for motion of anions,  $\Delta V_m^-$ , is much greater than that for cations. It would be desirable to measure  $\Delta V_m^-$  for these systems. Such a measurement will also provide a test for Flynn's prediction<sup>3</sup> that  $\Delta V_m^+/\Delta V_m^- = \Delta G_m^+/\Delta G_m^-$ .

The observed activation volumes for motion of cations agree well with predictions of the strain-energy model of Keyes<sup>1</sup> and the dynamical theory of Flynn,<sup>2,3</sup> if the observed pressure dependence of the effective shear modulus is used. The observed pressure dependence of the long-wavelength transverse-optical-mode frequencies shows a poor correlation with the observed  $\Delta V_m^+$ , possibly because the contributions of other more important optic modes have not been included.

The uncertainty in the estimated formation volume  $\Delta V_f$  of Schottky defects is high in the present analysis. Although the experimental errors are no higher than those in previous measurements, the inclusion of anion and extrinsic vacancy contributions causes large uncertainties. However, despite these larger uncertainties, the values deduced for  $\Delta V_f$  are still appreciably larger than those calculated by atomic models.

## ACKNOWLEDGMENTS

The authors benefited greatly from discussions with Dr. A. B. Lidiard, Dr. R. Jeffery, Dr. M. Beyeler, Professor C. P. Flynn, and M. Jackson.

†Research supported in part by the U. S. Atomic Energy Commission under Contract No. AT(11-1)-1198, and in

part by the U. S. National Science Foundation under Grant No. GK 5833.

\*Present address: Korea Advanced Institute of Science, P.O. Box 150, Chungryang-ri, Seoul, Korea.

<sup>1</sup>For a review of this subject, see articles by D. Lazarus and R. W. Keyes, in *Solids Under Pressure*, edited by W. Paul and D. M. Warschauer (McGraw-Hill, New York, 1963).

<sup>2</sup>C. P. Flynn, *Phys. Rev.* **171**, 682 (1968).

<sup>3</sup>C. P. Flynn, *Z. Naturforsch.* **26a**, 99 (1971); *Point Defects and Diffusion* (Oxford U.P., Oxford, England, 1972), Chap. 9.

<sup>4</sup>I. D. Faux and A. B. Lidiard, *Z. Naturforsch.* **26a**, 62 (1971).

<sup>5</sup>W. Biermann, *Z. Physik. Chem. (Frankfurt)* **25**, 90 (1960); **25**, 253 (1960).

<sup>6</sup>C. B. Pierce, *Phys. Rev.* **123**, 253 (1960).

<sup>7</sup>W. H. Taylor II, N. B. Daniels, B. S. H. Royce, and R. Smoluchowski, *J. Phys. Chem. Solids* **27**, 39 (1966).

<sup>8</sup>M. Beyeler and D. Lazarus, *Solid State Commun.* **7**, 1487 (1969).

<sup>9</sup>M. Beyeler and D. Lazarus, *Z. Naturforsch.* **26a**, 291 (1971).

<sup>10</sup>D. Lazarus, D. N. Yoon, and R. N. Jeffrey, *Z. Naturforsch.* **26a**, 56 (1971).

<sup>11</sup>R. M. Emrick, *Phys. Rev.* **122**, 1720 (1961).

<sup>12</sup>D. Yoon, thesis (Harvard University, 1967) (unpublished).

<sup>13</sup>For more detailed data, see Ref. 10.

<sup>14</sup>D. Miliotis and D. N. Yoon, *J. Phys. Chem. Solids* **30**, 1241 (1969).

<sup>15</sup>R. G. Fuller *et al.*, *Phys. Rev. Letters* **20**, 662 (1968).

<sup>16</sup>K. Kobayashi and T. Tomiki, *J. Phys. Soc. Japan* **15**, 1982 (1960).

<sup>17</sup>See A. B. Lidiard, in *Handbuch der Physik*, edited by S. Flügge (Springer, Berlin, 1957), Vol. 20, p. 246.

<sup>18</sup>D. Enck, *Phys. Rev.* **119**, 1873 (1960).

<sup>19</sup>L. Hunter and S. Siegel, *Phys. Rev.* **61**, 84 (1942).

<sup>20</sup>S. P. Nikanaorov and A. V. Stepanov, *Zh. Eksperim. i Teor. Fiz.* **37**, 1814 (1959) [*Sov. Phys. JETP* **10**, 1280 (1959)].

<sup>21</sup>R. W. Roberts and C. S. Smith, *J. Phys. Chem. Solids* **31**, 619 (1970).

<sup>22</sup>D. Lazarus, *Phys. Rev.* **76**, 545 (1949); R. A. Bertels and D. E. Schuele, *J. Phys. Chem. Solids* **26**, 537 (1965).

<sup>23</sup>P. J. Reddy and A. L. Ruoff, in *Physics of Solids at High Pressure*, edited by C. T. Tomizuka and R. M. Emrick (Academic, New York, 1965), p. 510.

<sup>24</sup>R. G. Fuller, *Phys. Rev.* **142**, 524 (1966).

<sup>25</sup>V. C. Nelson and R. J. Friauf, *J. Phys. Chem. Solids* **31**, 825 (1970).

<sup>26</sup>J. Rolfe, *Can. J. Phys.* **42**, 2195 (1964).

<sup>27</sup>M. P. Tosi and F. G. Fumi, *J. Phys. Chem. Solids* **25**, 31 (1964); **25**, 45 (1964).

<sup>28</sup>B. Fritz, F. Luty, and J. Anger, *Z. Physik* **174**, 240 (1963).

<sup>29</sup>C. Zener, *Acta Cryst.* **2**, 163 (1949).

<sup>30</sup>H. Brooks, *Impurities and Imperfections* (American Society for Metals, Cleveland, 1955).

<sup>31</sup>L. W. Barr and A. B. Lidiard, *Physical Chemistry, an Advanced Treatise* (Academic, New York, 1970), Vol. 10.

<sup>32</sup>S. A. Rice, *Phys. Rev.* **112**, 804 (1958); O. P. Manley, *J. Phys. Chem. Solids* **32**, 1046 (1960).

<sup>33</sup>C. Postmus, J. R. Ferraro, and S. S. Mitra, *Phys. Rev.* **174**, 983 (1968).

<sup>34</sup>For a brief review, see Ref. 4.

## Radiation-Induced $[\text{Na}]^0$ Centers in MgO and $\text{SrO}^\dagger$

M. M. Abraham, Y. Chen, J. L. Kolopus,\* and H. T. Tohver<sup>‡</sup>

*Solid State Division, Oak Ridge National Laboratory, Oak Ridge, Tennessee 37830*

(Received 9 February 1972)

Substitutional monovalent sodium ions in MgO and SrO trap holes when exposed to ionizing radiation at 77 K. The  $[\text{Na}]^0$  centers thus formed have  $\langle 100 \rangle$  axial symmetry at 4.2 K and their spin-Hamiltonian parameters are reported. The isotropic part of the hyperfine interaction for  $[\text{Na}]^0$ , which has opposite sign to the anisotropic term, is larger than that observed for  $[\text{Li}]^0$  in these hosts. Optical absorption bands have been correlated with the  $[\text{Na}]^0$  centers, and their peaks occur at 1.58 eV for MgO and 1.34 eV for SrO. Decay temperatures have been determined to be approximately 190 K for MgO and 160 K for SrO. The EPR, optical, and thermal properties of these centers resemble those of the  $V^-$  and  $[\text{Li}]^0$  centers.

### INTRODUCTION

During irradiation a cation vacancy in the alkaline earth oxides can trap a hole and form the paramagnetic  $V^-$  center.<sup>1-3</sup> The center has been identified by EPR studies to have axial symmetry along the  $\langle 100 \rangle$  direction, with the hole preferentially located at one of the neighboring oxygen sites, forming an

$\text{O}^-$  ion, at any given time. In the case of MgO, an optical absorption band peaking at 2.3 eV has been correlated with the  $V^-$  center.<sup>4,5</sup> The half-width of the band,  $\sim 1$  eV, is exceptionally large and the oscillator strength of  $\sim 0.1$  reflects neither a purely allowed nor a purely forbidden transition.

A monovalent alkali ion placed at a cation vacancy can also capture a hole during irradiation to form